Eur. Phys. J. A **21**, 1–6 (2004)
DOI 10.1140/epja/i2004-10034-8

THE EUROPEAN PHYSICAL JOURNAL A

Letter

Investigation of lifetimes in dipole bands of ^{141}Eu

E.O. Podsvirova[1,2], R.M. Lieder[1,a], A.A. Pasternak[1,2], S. Chmel[3], W. Gast[1], Ts. Venkova[1,4], H.M. Jäger[1], L. Mihailescu[1], G. de Angelis[5], D.R. Napoli[5], A. Gadea[5], D. Bazzacco[6], R. Menegazzo[6], S. Lunardi[6], W. Urban[7], Ch. Droste[7], T. Morek[7], T. Rząca-Urban[7], and G. Duchêne[8]

[1] Institut für Kernphysik, Forschungszentrum Jülich, D-52425 Jülich, Germany
[2] A.F. Ioffe Physical Technical Institute RAS, RU-194021 St. Petersburg, Russia
[3] Institut für Strahlen- und Kernphysik, University of Bonn, D-53115 Bonn, Germany
[4] Institute of Nuclear Research and Nuclear Energy, Bulgarian Academy of Sciences, BG-1784 Sofia, Bulgaria
[5] Istituto Nazionale di Fisica Nucleare, Laboratori Nazionali di Legnaro, I-35020 Legnaro, Italy
[6] Dipartimento di Fisica dell'Università and Istituto Nazionale di Fisica Nucleare, Sezione di Padova, I-35131 Padova, Italy
[7] Institute of Experimental Physics, University of Warsaw, PL-00-681 Warszawa, Poland
[8] Institut de Recherches Subatomique IReS, F-67037 Strasbourg, France

Received: 6 April 2004 / Revised version: 14 May 2004 /
Published online: 13 July 2004 –
Communicated by D. Schwalm

Abstract. Lifetimes have been measured for dipole bands in ^{141}Eu using DSAM. The deduced $B(M1)$ and $B(E2)$ values as well as $B(M1)/B(E2)$ ratios are compared with calculations in the framework of the TAC (Tilted Axis Cranking) and SPAC (Shears mechanism with Principal Axis Cranking) models. The dipole bands can be interpreted as magnetic rotational bands.

PACS. 21.10.-k Properties of nuclei; nuclear energy levels – 21.10.Re Collective levels – 21.10.Tg Lifetimes – 27.60.+j $90 \leq A \leq 149$

1 Introduction

The existence of regular rotational bands, consisting of strong magnetic dipole transitions, in nearly spherical nuclei is well established [1–3]. These bands have been interpreted as resulting from the coupling of the angular momentum vectors $\boldsymbol{j}_1$ and $\boldsymbol{j}_2$ of a few high-j particles of one kind and high-j holes of the other kind of nucleons, respectively, oriented approximately perpendicular to each other at the band head, for generating the total spin of the nucleus [3]. This coupling results in a substantial component of the magnetic dipole moment which is transverse to the total spin. As this component of the magnetic dipole moment rotates around the vector of the total angular momentum this new mode has been called "Magnetic Rotation" (MR) [3]. The angular momentum of the band is increased by the gradual alignment of the individual nucleon spins along the total-angular-momentum vector. This way of angular-momentum production has been called "shears mechanism". The MR bands have very large $B(M1)$ values (several μ_N^2) and their crossover transitions, if existent at all, have very small $B(E2)$ values ($\approx 0.1(eb)^2$). Because of the alignment of the nucleons the $B(M1)$ values are decreasing with increasing spin.

Magnetic rotations are expected in regions close to magic numbers if high-j nucleons are available and the deformation is small [3]. Also for the $N \approx 82$ region MR bands are predicted and four dipole bands have been found in the nucleus ^{142}Gd [4] which were considered as MR bands from a comparison of the frequency dependence of their angular momenta I and their ratios of reduced transition probabilities $B(M1)/B(E2)$ with predictions of the Tilted Axis Cranking (TAC) model [3]. The dipole bands DB1 and DB2 in ^{142}Gd may have $\pi h_{11/2}^2 \otimes \nu h_{11/2}^{-2}$ and $\pi h_{11/2}^2 \otimes \nu h_{11/2}^{-4}$ configurations [4]. The previously observed dipole bands in ^{141}Eu [5] have a similar frequency dependence of the angular momentum as the above-mentioned dipole bands in ^{142}Gd, except that the angular momentum is shifted in ^{141}Eu by $\approx 2\ \hbar$ to lower values. Their configurations may result from those of the dipole bands DB1 and DB2 in ^{142}Gd by subtraction of an $h_{11/2}$ proton. A proof for the interpretation of the dipole bands in ^{141}Eu as MR bands may result from lifetime measurements and

[a] e-mail: r.lieder@fz-juelich.de

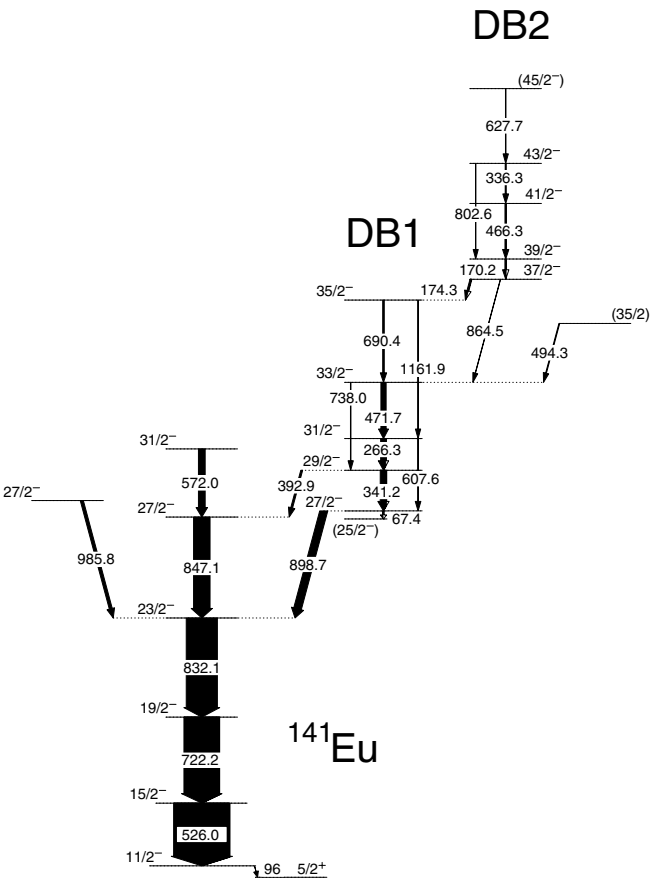

Fig. 1. Partial level scheme of ^{141}Eu showing the dipole bands DB1 and DB2. The widths of the arrows represent the intensities of the transitions.

the determination of $B(M1)$ and $B(E2)$ values as well as a comparison with calculations in the framework of the TAC (Tilted Axis Cranking) and the semiclassical SPAC (Shears mechanism with Principal Axis Cranking) models. A preliminary report on the present investigation has been given in ref. [6].

2 Experimental methods and results

High-spin states in ^{141}Eu have been studied with EUROBALL III [7] using the ^{99}Ru(^{48}Ti, 3p3n) reaction at a beam energy of 240 MeV. In this investigation ^{142}Gd was populated through the 2p3n channel with 27% of the total fusion cross-section and the experiment is described fully in ref. [4]. The nucleus ^{141}Eu is produced with a relative cross-section of 9%. The experiment was carried out at the XTU tandem —linear accelerator (ALPI) combination of the Laboratori Nazionali di Legnaro, Italy. To allow for an isotopic separation and to increase thus the selectivity of EUROBALL III the charged-particle detector array ISIS, consisting of 40 Si detector telescopes, was mounted in the center of the γ-detector array [8]. The ^{99}Ru target, enriched to 95%, consisted of four self-supporting metal foils with a total thickness of 0.84 mg/cm^2. Approximately

Table 1. $B(M1)/B(E2)$ ratios, lifetimes, $B(M1)$ and $B(E2)$ values for the dipole bands DB1 and DB2 of ^{141}Eu.

I_i^π	$\frac{B(M1)}{B(E2)}$ $(\mu_N/eb)^2$	τ (ps)	$B(M1)$ (μ_N^2)	$B(E2)$ $(10^{-2}\ e^2b^2)$
$29/2^-$		$1.1^{+0.4}_{-0.3}$	$0.79^{+0.51}_{-0.14}$	
$31/2^-$	17^{+3}_{-2}	$2.5^{+1.0}_{-0.5}$	$0.75^{+0.38}_{-0.15}$	$4.1^{+2.3}_{-0.9}$
$33/2^-$	16^{+8}_{-3}	$1.1^{+0.4}_{-0.3}$	$0.37^{+0.24}_{-0.06}$	$2.3^{+1.7}_{-0.5}$
$35/2^-$	11^{+3}_{-1}			
$37/2^-$	299^{+178}_{-54}			
$41/2^-$	$\geq 17^{(a)}$	$0.55^{+0.25}_{-0.20}$	$0.77^{+0.76}_{-0.13}$	$\leq 4.5^{(a)}$
$43/2^-$	17^{+15}_{-2}	0.8 ± 0.2	$1.32^{+0.69}_{-0.22}$	$6.4^{+4.1}_{-2.0}$
$45/2^-$		$0.29^{+0.20}_{-0.15}$	$0.50^{+0.84}_{-0.07}$	

(^{a}) Obtained from the intensity limit for a 68% confidence interval.

$4.5 \cdot 10^9$ high-fold γ events have been collected, $\approx 60\%$ of which were associated with one or more detected particles. Details of the data analysis, carried out with the software package "Ana" [9], are described in ref. [4]. Two γ-γ-γ cubes gated on one and two protons, respectively, have been used for the investigation of the ^{141}Eu level scheme. The former cube has mainly been used for the analysis since it has about a factor of two more events associated with ^{141}Eu than the latter, although it is less clean.

A partial level scheme of ^{141}Eu obtained from this work is shown in fig. 1. It agrees with previous level schemes [5,10] except for dipole band DB2 for which the order of the 336.3 and 466.3 keV lines has been inverted using lifetime (see below) and intensity arguments. The latter line is $\approx 50\%$ stronger than the former one. With respect to ref. [5] the energy of the $(45/2^-) \rightarrow (43/2^-)$ transition was found to be 627.7 keV and three additional crossover transitions have been placed in the dipole bands DB1 and DB2. A $(41/2^-) \rightarrow (37/2^-)$ crossover transition of 636.5 keV has not been found, its intensity being $\lesssim 3\%$ of that of the dipole transition de-exciting the same level. The DCO ratios of the 341.2, 266.3, 471.7, 174.3, 170.2, 466.3 and 336.3 keV transitions, obtained by gating on low-lying stretched $E2$ transitions, range between 0.3 and 0.6 indicating mixed $M1/E2$ character with a spin change of $\Delta I = 1$. The spin-parity assignments given in fig. 1 are based on these results. Taking into account the $B(M1)/B(E2)$ ratios presented in table 1, the 174.3 and 864.5 keV transitions are considered to connect the dipole bands DB1 and DB2, since the $B(M1)/B(E2)$ ratio is more than one order of magnitude larger than those found for the other $M1$ and $E2$ transitions.

With EUROBALL IV at IReS Strasbourg a lifetime experiment using the Doppler-Shift Attenuation Method (DSAM) has been carried out which allowed to determine the $B(M1)$ and $B(E2)$ values of the dipole bands DB1

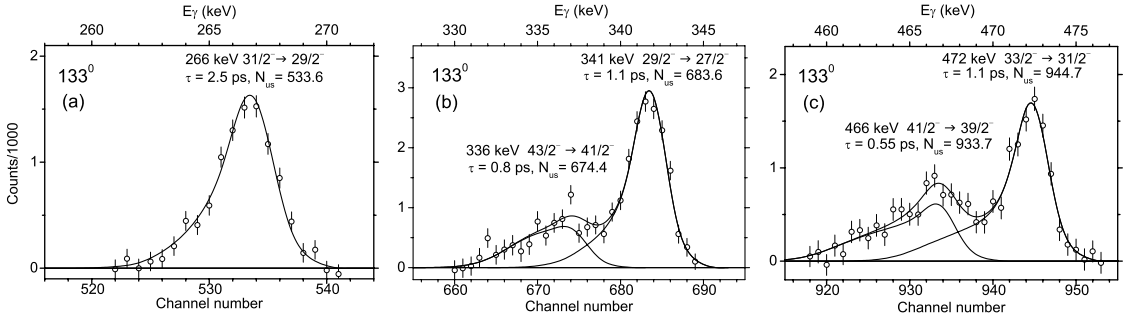

Fig. 2. Lineshape analysis for the 266.3 keV line and the 336.3-341.2 keV and 466.3-471.7 keV doublets of the dipole bands DB1 and DB2 in ^{141}Eu. The lifetimes have been obtained in a χ^2 analysis.

and DB2 in ^{141}Eu. To minimize the sidefeeding lifetimes, a ^{114}Sn target was bombarded with ^{32}S projectiles of 160 MeV. The final nucleus is produced in the 3p2n reaction channel. As target a self-supporting metallic ^{114}Sn foil of 8 mg/cm^2 thickness with an enrichment of 71.1% has been used. The initial recoil velocity is $v/c = 2.2\%$ for this reaction. EUROBALL IV (consisting of 14 CLUSTER, 26 CLOVER and 30 individual Compton-suppressed Ge detectors) was equipped with an inner BGO ball and the particle detector array EUCLIDES. Events were recorded when ≥ 5 unsuppressed Ge detectors fired in coincidence. Approximately $4.3 \cdot 10^9$ high-fold γ events have been collected. The energy and efficiency calibrations of EUROBALL IV have been carried out with a ^{152}Eu source.

To extract lifetimes the data have been sorted into several γ-γ-γ cubes for which the γ-ray energies from any detector were stored into the first two axes and the energies from detectors placed under a certain angle with respect to the beam direction in the third axis of the respective cube. The DSAM lineshape analysis was hence carried out in doubly gated coincidence spectra. The detector rings at average angles of 133° (10 CLUSTER detectors), 103° (13 CLOVER detectors) and 77° (13 CLOVER detectors) have been used because the corresponding spectra have the highest statistics. These cubes contain $54 \cdot 10^9$, $54 \cdot 10^9$ and $59 \cdot 10^9$ γ-γ-γ events, respectively. The energy and time calibrations, the presort and the sort of the γ-γ-γ cubes have been carried out with the software package *Ana* [9]. Since the instrumental lineshapes and efficiencies, respectively, of the various detector rings differ from each other, they have been determined separately for each ring.

The analysis of experimental DSAM lineshapes was carried out using updated versions of the Monte Carlo codes COMPA, GAMMA and SHAPE [11]. The "wide gate below" technique has been applied to obtain sufficient statistics in the analysed spectra. Therefore, sidefeeding has to be taken into account. The time distributions of the sidefeeding have been calculated with Monte Carlo methods and the relevant parameters were determined by the investigation of γ-ray multiplicity spectra for $^{142-146}$Gd [12]. In some cases the spectra for the symmetric angles of 77° and 103° have been added to improve the statistics. The resulting DSAM lineshapes are then symmetric. The uncertainties result from statistical contributions and from uncertainties related to the cascade- and side-feeding pattern as well as from the uncertainty of the stopping power for the recoils. The statistical uncertainties are obtained by a χ^2 analysis taking into account the variable parameters of all peaks in the fitted multiplet. Intensities, important for taking into account cascade feeding, have been evaluated from the fit of the DSAM lineshapes in the spectra. They are in agreement with the intensities obtained in the EUROBALL III experiment.

Lifetimes have been deduced for three levels in each of the dipole bands DB1 and DB2 of ^{141}Eu. The DSAM lineshape analysis for the 266.3 keV line and the 336.3-341.2 keV and 466.3-471.7 keV doublets is shown in fig. 2. The spectra result from the 133° CLUSTER-detector ring and were obtained by summing various clean gate combinations. For the 266.3 keV line (fig. 2a), transitions lying below the $29/2^-$ level have been used for gating. The full line shows the result of the lineshape analysis. In figs. 2b, c gates have been placed below the $39/2^-$ level to enhance the statistics for the 336.3 and 466.3 keV transitions in DB2. First, the lifetimes for the levels de-excited by these γ-rays were determined as shown in figs. 2b, c. Subsequently, the lifetimes for the levels de-excited by the 341.2 and 471.7 keV transitions in DB1 were determined from other spectra including only gate combinations of transitions lying below the $27/2^-$ level by fixing the lifetimes for the 336.3 and 466.3 keV lines. The unshifted peak positions of the transitions $N_{\rm us}$ (given in channels in fig. 2) were fixed for all peaks and they have been determined in spectra obtained by adding those for the 77° and 103° CLOVER rings because these spectra show symmetric lineshapes and the Doppler effects are smaller. To confirm the order of the 466.3 and 336.3 keV transitions shown in the level scheme of fig. 1, the lifetimes have also been determined for the reversed order. Whereas the lifetime of the level de-excited by the 466.3 keV line did not change very much, a lifetime of $\tau \leq 0.05$ ps would result for the 336.3 keV transition. This is an unreasonable value since the corresponding $B(M1)$ value would be ≈ 20 times larger than all other $B(M1)$ values of DB1 and DB2 (cf. table 1) confirming the present ordering of these transitions.

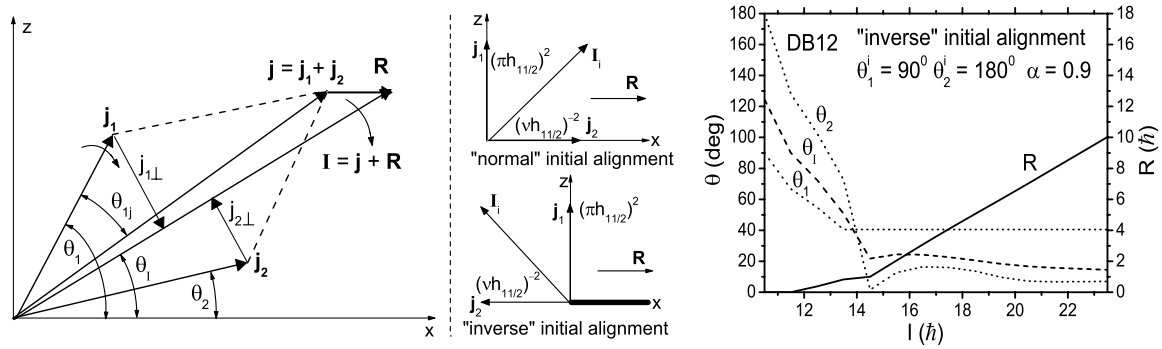

Fig. 3. Left portion: angular momentum coupling scheme used in the SPAC model. Middle portion: two different initial orientations of the angular momentum $\boldsymbol{j}_2$ are depicted. Right portion: evolution of the angles θ_1, θ_2, θ_I and the rotational angular-momentum vector R with spin for the "inverse" initial alignment for the dipole bands DB1 and DB2 in ^{141}Eu.

The lifetimes and the deduced $B(M1)$, $B(E2)$ and $B(M1)/B(E2)$ values are given in table 1. The $B(M1)$, $B(E2)$ and $B(M1)/B(E2)$ values and their uncertainties have been calculated with Monte Carlo methods since the errors of the lifetimes and intensities are large and the application of the error propagation law underestimates the uncertainties. In the Monte Carlo simulations the probability distributions for the resulting quantities have been calculated assuming Gaussian probability distributions for the lifetimes and intensities. The resulting probability distributions are not any more Gaussian and the most probable $B(M1)$, $B(E2)$ and $B(M1)/B(E2)$ values, respectively, are taken with uncertainties reflecting a 68% confidence interval. The most probable values deviate from the median values which equal the values obtained using the well-known equations for these quantities. Taking the example of the $43/2^-$ level with a lifetime $\tau = 0.8 \pm 0.2$, de-excited by the 336.3 keV and 802.6 keV transitions with relative intensities $I_\gamma = 2.7 \pm 0.3$ and 0.8 ± 0.3, respectively, one finds for the 336.3 keV transition a median value $B(M1) = 1.44 \pm 0.42$, using the error propagation law to calculate the uncertainty. The most probable value, however, is $B(M1) = 1.32^{+0.69}_{-0.22}$ (given in table 1) where the uncertainties reflect the 68% confidence interval. The corresponding values for the $B(M1)/B(E2)$ ratio, which is an independent quantity because it results from the branching ratio, are 20 ± 8 and 17^{+15}_{-2}, respectively.

3 Discussion

Calculations have been carried out in the framework of the TAC model [3] and a semiclassical model similar to the Clark and Macchiavelli approach [2]. A few semiclassical scenarios are in use to calculate the features of dipole bands. In the limiting case, when the angular-momentum vectors of the involved particles and holes $\boldsymbol{j}_1$ and $\boldsymbol{j}_2$ are aligned along the symmetry (z) and rotation (x) axes, respectively, considered in the framework of the Principal Axis Cranking (PAC) coupling scheme [13], the angular-momentum vector $\boldsymbol{R}$ of the collective rotation is parallel to the x-axis. In the case when the total spin is produced solely by the shears effect and the collective rotation is absent, only the angle between the angular-momentum vectors $\boldsymbol{j}_1$ and $\boldsymbol{j}_2$ is of importance and a semiclassical description is possible [2]. Collective rotation has been added to this model [14] in the framework of a coupling scheme, in which the vectors $\boldsymbol{R}$ and $\boldsymbol{j} = \boldsymbol{j}_1 + \boldsymbol{j}_2$ are parallel to each other.

In the present work another approach has been chosen in which the shears mechanism is combined with PAC and this semiclassical model has been called SPAC model. The vector coupling scheme is depicted in the left portion of fig. 3. The total energy contains collective and quasiparticle contributions: $E(I,\theta_1,\theta_2) = 1/(2J)\ R^2(I,\theta_1,\theta_2) + V_2\ P_2(\theta_1-\theta_2) + \text{const}$, where $P_2(\theta_1-\theta_2) = [3\cos^2(\theta_1-\theta_2)-1]/2$ and $R(I,\theta_1,\theta_2) = \sqrt{I^2-(j_1\sin\theta_1 + j_2\sin\theta_2)^2} - j_2\cos\theta_2 - j_1\cos\theta_1$. Generally, for each value of I the angles $\theta_1(I)$ and $\theta_2(I)$ can be found from the minimization condition $\left(\frac{\partial^2 E}{\partial\theta_1\partial\theta_2}\right)_I = 0$. Subsequently, the total energy $E(I)$ and transition probabilities can be caclulated as functions of I. Taking into account the classical approximation of Clebsch-Gordon coefficients the reduced $M1$ transition probability [2] is $B(M1;I\to I-1) = \frac{3}{8\pi}\mu_\perp^2$, with $\mu_\perp = g_1^*\ j_{1\perp} - g_2^*\ j_{2\perp}$, $j_{1\perp} = j_1\sin(\theta_1-\theta_I)$, $j_{2\perp} = j_1\sin(\theta_I-\theta_2)$, $g_1^* = g_1 - g_R$, $g_2^* = g_2 - g_R$ and $g_R = Z/A$. The reduced $E2$ transition probability is $B(E2;I\to I-2) = \frac{15}{128\pi}[Q_{\text{eff}}\sin^2\theta_{1j} + Q_{\text{coll}}\cos^2\theta_I]^2$, where Q_{eff} and Q_{coll} are quasiparticle and collective transitional quadrupole moments. The latter quadrupole moment and the collectivity parameter $C = 1/(2J)$ of the core are assumed to be I dependent and have been described in the band crossing region by the Boltzmann functions: $C(I) = C_{\text{f}} + (C_{\text{i}} - C_{\text{f}})/\{1+\exp[(I-I_{\text{tr}})/\Delta]\}$ and $Q_{\text{coll}}(I) = Q_{\text{f}} + (Q_{\text{i}} - Q_{\text{f}})/\{1+\exp[(I-I_{\text{tr}})/\Delta]\}$, i and f denoting the initial and final values and I_{tr} the spin at which the crossing takes place.

Generally, any initial orientation of the angular-momentum vectors $\boldsymbol{j}_1$ and $\boldsymbol{j}_2$ can be considered. Particularly, the two symmetric initial orientations of $\boldsymbol{j}_2$, resulting from a rotation by $\Re_z(\pi)$, generate three different dipole bands. The corresponding alignment schemes are shown in the middle portion of fig. 3 and are labelled "normal"

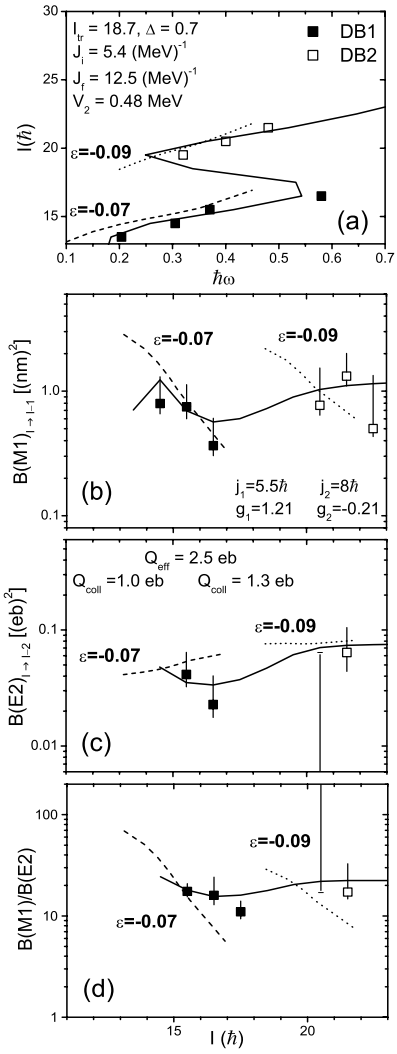

Fig. 4. Comparison of experimental results for the dipole bands DB1 (full squares) and DB2 (open squares) in ^{141}Eu with those of calculations in the framework of the TAC and SPAC models: (a) angular momentum I *vs.* rotational frequency $\hbar\omega$, (b) $B(M1)$ values, (c) $B(E2)$ values, (d) $B(M1)/B(E2)$ ratios. The TAC calculations are shown as dashed lines for DB1 ($\epsilon_2 = -0.07$) and as dotted lines for DB2 ($\epsilon_2 = -0.09$). SPAC results for the "inverse" initial alignment are shown as full lines.

and "inverse" initial alignment. For the latter case a clockwise rotation of the total angular momentum is considered but a counterclockwise rotation is also possible. In case of the normal initial alignment $\theta_2 = 0$, and $\theta_1(I)$ can be found applying the one-dimensional minimization condition $\left(\frac{\mathrm{d}E}{\mathrm{d}\theta_1}\right)_I = 0$. For the inverse initial alignment the required two-dimensional search of the energy minimum can be replaced by the one-dimensional minimization condition $\left(\frac{\mathrm{d}E}{\mathrm{d}\theta_2}\right)_I = 0$ if, before the crossing of θ_1 and θ_2, the dependence of θ_1 on θ_2 is described as $\theta_1(\theta_2) = \theta_1^i \cdot (\theta_2/\theta_2^i)^\alpha$ and after the crossing θ_1 is fixed. The parameter α describes the differences in the spin dependences of the angles θ_1 and θ_2. It turned out that the dipole band based on the inverse initial alignment is energetically favoured as compared to the normal one. For the inverse solution, the evolution of the angles θ_1, θ_2, θ_I as well as R as a function of spin is shown in the right portion of fig. 3.

In fig. 4 the experimental results for the dipole bands in ^{141}Eu are compared with calculations in the framework of the TAC and SPAC models. In this figure the angular momentum I is plotted *vs.* the rotational frequency $\hbar\omega$ (fig. 4a) and $B(M1)$ (fig. 4b) and $B(E2)$ (fig. 4c) values as well as $B(M1)/B(E2)$ ratios (fig. 4d) are plotted as a function of spin. For the TAC model calculations a similar parameter set as for ^{142}Gd [4] has been used. Pairing is taken into account by using gap energies $\Delta_\pi = 1.16$ MeV and $\Delta_\nu = 0.59$ MeV as deduced from 80% of the odd-even mass differences. For the dipole bands DB1 and DB2 in ^{141}Eu $\pi h^1_{11/2} \otimes \nu h^{-2}_{11/2}$ and $\pi h^1_{11/2} \otimes \nu h^{-4}_{11/2}$ configurations, respectively, have been assumed. The same configuration has also been previously assigned to DB1 [15]. The results of the TAC model calculations for DB1 and DB2 using $\varepsilon_2 = -0.07$ and -0.09 ($\varepsilon_4 = 0$ and $\gamma = 0$), respectively, are included in fig. 4. It is expected that the alignment of a second $\nu h_{11/2}$ hole pair causes an increase of the deformation suggesting that the deformation for DB2 is larger than for DB1. The deformations have been chosen to reproduce the experimental $B(E2)$ values. The TAC model calculations can quite well reproduce the experimental results. Results of the SPAC model calculations for the inverse initial alignment are shown in fig. 4. At the spin $I_{\mathrm{tr}} = 18.7$ (cf. fig. 4a) an increase of the collectivity, implying a structural change, is assumed which allows to explain the backbending between DB1 and DB2, seen in fig. 4a. Also calculations assuming a band crossing have been made with the SPAC model taking into account band mixing [16] but they cannot as well describe the experimental results. The good agreement between the experimental results and those of the TAC and SPAC model calculations indicates that the dipole bands in ^{141}Eu can indeed be considered as magnetic rotational bands.

4 Summary

Lifetimes have been measured for ^{141}Eu using DSAM. The experiment has been carried out with EUROBALL IV employing the ^{114}Sn(^{32}S, 3p2n) reaction at a beam energy of 160 MeV. Level scheme information resulted from an EUROBALL III experiment using the ^{99}Ru(^{48}Ti, 3p3n) reaction at a beam energy of 240 MeV. Lifetimes have been determined for three levels in each of the dipole bands of ^{141}Eu. The deduced $B(M1)$ and $B(E2)$ values as well as $B(M1)/B(E2)$ ratios are compared with calculations in the framework of the microscopic TAC (Tilted Axis Cranking) and semiclassical SPAC (Shears mechanism with Principal Axis Cranking) models. The dipole bands can be interpreted as magnetic rotational bands considering the good agreement between experiment and calculations.

We are grateful to the accelerator crews in Legnaro and Strasbourg for providing the beam and to the EUROBALL crew for technical support. The work was partly supported by the Heinrich Hertz Foundation, Germany under the contract No. 16/03, by the IB of BMBF at DLR, Germany under the WTZ contract RUS 99/191 and by the EU under the TMR contract ERBFMRXCT970123 and the LSF contract HPRI-CT-1999-00078. Enlightening discussions with S. Frauendorf and H. Hübel on the SPAC model are gratefully acknowledged.

References

1. H. Hübel *et al.*, Z. Phys. A **358**, 237 (1997).
2. R.M. Clark, A.O. Macchiavelli, Annu. Rev. Nucl. Part. Sci. **50**, 36 (2000).
3. S. Frauendorf, Rev. Mod. Phys. **73**, 463 (2001).
4. R.M. Lieder *et al.*, Eur. Phys. J. A **13**, 297 (2002).
5. N. Xu *et al.*, Phys. Rev. C **43**, 2189 (1991).
6. R.M. Lieder *et al.*, *Proceedings of the International Conference on The Labyrinth in Nuclear Structure, Crete, Greece*, edited by A. Bracco, C.A. Kalfas, AIP Conf. Proc. **701**, 238 (2004).
7. R.M. Lieder, in *Experimental Techniques in Nuclear Physics*, edited by D.N. Poenaru, W. Greiner (Walter de Gruyter, Berlin, 1997) p. 137.
8. E. Farnea *et al.*, Nucl. Instrum. Methods A **400**, 87 (1997).
9. W. Urban, Manchester University, Nuclear Physics Report 1991-1992, p. 95.
10. Z. Marcinkowska *et al.*, Acta Physica Pol. B **34**, 2319 (2003).
11. R.M. Lieder *et al.*, this issue, p. 37.
12. A.A. Pasternak *et al.*, Laboratori Nazionali di Legnaro Annu. Rep. 2001, p. 44, web edition: `www.lnl.infn.it`; *Investigation of fold distributions for residual nuclei produced in the* $^{114}Cd+\,^{36}S$, $^{100}Mo+\,^{48}Ti$ *and* $^{97}Mo+\,^{51}V$ *reactions*, to be published in Eur. Phys. J. A.
13. F. Dönau, S. Frauendorf, *Proceedings of the Conference on High Angular Momentum Properties of Nuclei, Oak Ridge, 1982*, edited by N.R. Johnson, Nucl. Sci. Res. Conf. Ser., Vol. **4** (Harwood, New York, 1983) p. 143.
14. A.O. Macchiavelli *et al.*, Phys. Lett. B **450**, 1 (1999).
15. H. Güven *et al.*, Z. Phys. A **330**, 437 (1988).
16. J.R. Cooper *et al.*, Phys. Rev. Lett. **87**, 132503 (2001).